POLITECNICO DI TORINO
Repository ISTITUZIONALE

Direct MT data transform into 1-D resistivity models: a new approach based on cumulative resistance models

Original
Direct MT data transform into 1-D resistivity models: a new approach based on cumulative resistance models / Hernandez, O., Rondoni, L., Slob, Evert., Socco, Laura.. - In: GEOPHYSICAL JOURNAL INTERNATIONAL. - ISSN 0956-540X. - 244:1(2026), pp. 1-7. [10.1093/gji/ggaf425]

Availability:
This version is available at: 11583/3005271 since: 2025-11-19T10:24:49Z

Publisher:
Oxford University Press

Published
DOI:10.1093/gji/ggaf425

Terms of use:

This article is made available under terms and conditions as specified in the corresponding bibliographic description in the repository

Publisher copyright

(Article begins on next page)

28 June 2026

Geophysical Journal International

Geophys. J. Int. (2025) **244,** 1–7
Advance Access publication 2025 October 23
Express Letter

https://doi.org/10.1093/gji/ggaf425

Direct MT data transform into 1-D resistivity models: a new approach based on cumulative resistance models

Oscar I. Calderon Hernandez [1], L. Rondoni,[2,3] E.C. Slob [4] and L. V. Socco[1,4]

[1] *Dipartimento di Ingegneria dell'Ambiente, del Territorio e delle Infrastrutture, Politecnico di Torino, Torino 10129, Italy. E-mail: oscar.calderon@polito.it*
[2] *Dipartimento di Scienze Matematiche 'G. L. Lagrange', Politecnico di Torino, Torino 10129, Italy*
[3] *Istituto Nazionale di Fisica Nucleare, Sezione di Torino, Torino 10125, Italy*
[4] *Faculty of Civil Engineering and Geosciences, Delft University of Technology, Delft 2628CN, the Netherlands*

Accepted 2025 October 19. Received 2025 October 16; in original form 2025 June 12

SUMMARY

Magnetotelluric (MT) data inversion seeks to recover resistivity models of the subsurface. Solving the inversion problem is a non-trivial task, as multiple plausible solutions can be recovered due to the nonlinearity of the problem. To reduce this nonlinearity, we propose a data-driven approach where a 1-D cumulative resistance model is estimated from MT data via a direct data transformation. We define the cumulative representation of layered models as the weighted sum of layer thickness divided by resistivity from surface to any depth level, which is the cumulative conductance. Its inverse, cumulative resistance, is directly related to the real part of the impedance computed from MT data. We train a neural network to transform the MT impedance into a resistance model. The corresponding 1-D resistivity model is obtained without *a priori* information. We validate our approach using synthetic and real data, opening the discussion for future developments of this new perspective.

Key words: North America; Magnetotellurics; Inverse Theory; Neural networks, fuzzy logic.

1 INTRODUCTION

The magnetotelluric method (MT) is a passive geophysical technique based on the measurement of the components of the electric and magnetic fields generated by an electromagnetic wave that travels through the structure of the Earth, and on the processing and inversion of these data to retrieve the resistivity distribution in the subsurface. For a layered Earth, Tikhonov (1965) derived the fundamentals of MT inversion theory by showing how the frequency dependence of the surface impedance determines the underlying conductivity structure. Afterwards, the theoretical uniqueness of MT 1-D inversion was demonstrated by Bailey (1970) for measurements in a continuum frequency space where no errors are present in the data. However, in reality, MT data measurements can be inaccurate and incomplete, which turns the inversion problem ill-posed and highly non-unique. To tackle this problem, two main approaches were proposed. The first was designed to retrieve the resistivity model directly from the data by using a data transform (Niblett & Sayn-Wittgenstein 1960; Jones & Foster 1986) exploiting the concepts of apparent resistivity and skin depth to provide a rough, first-approximation 1-D model of the subsurface. The second approach solved the inversion problem by an iterative forward modelling process (Constable *et al.* 1987; Zhang & Paulson 1997; Grandis *et al.* 1999; Trainor-Guitton & Hoversten 2011; Wang *et al.* 2022; Rodriguez *et al.* 2023), which typically relies on *a priori* constraints to reduce the solution space; furthermore, these techniques can be susceptible to convergence issues, particularly in the presence of noise or limited prior information. To address these limitations, recent studies for other geophysical methods (Socco & Comina 2015; Socco *et al.* 2017; Florio 2018) have solved the inversion problem by transforming the data directly into a cumulative model of the subsurface.

Inspired by this idea, in this work, our objective is to create a method for the direct transformation of MT data into a 1-D cumulative resistance model of the subsurface. By transforming the 1-D layered resistivity model into a 1-D cumulative resistance model we incorporate the influence of overlying layers into the model of the subsurface, a concept that is closely related to the nature of the geophysical measurements, which are inherently cumulative. We then retrieve a relationship between the cumulative model and the data in a fully data-driven approach without the need for concepts of apparent resistivity or skin depth. Once this relationship is established the MT data are transformed into a 1-D resistance model and an interval 1-D resistivity model is retrieved by applying the discrete derivative of the equation used to create the cumulative resistance model.

In this work we will focus on the 1-D case. Starting from MT data along with a cumulative 1-D resistance model, we established a model-data relationship that was used to train a mapping neural network to directly transform MT data into 1-D resistivity models. Afterwards, the trained network was used to directly transform unseen synthetic and real MT data into cumulative resistance models

© The Author(s) 2025. Published by Oxford University Press on behalf of The Royal Astronomical Society. This is an Open Access article distributed under the terms of the Creative Commons Attribution License (https://creativecommons.org/licenses/by/4.0/), which permits unrestricted reuse, distribution, and reproduction in any medium, provided the original work is properly cited.

Downloaded from https://academic.oup.com/gji/article/244/1/ggaf425/8300377 by guest on 19 November 2025

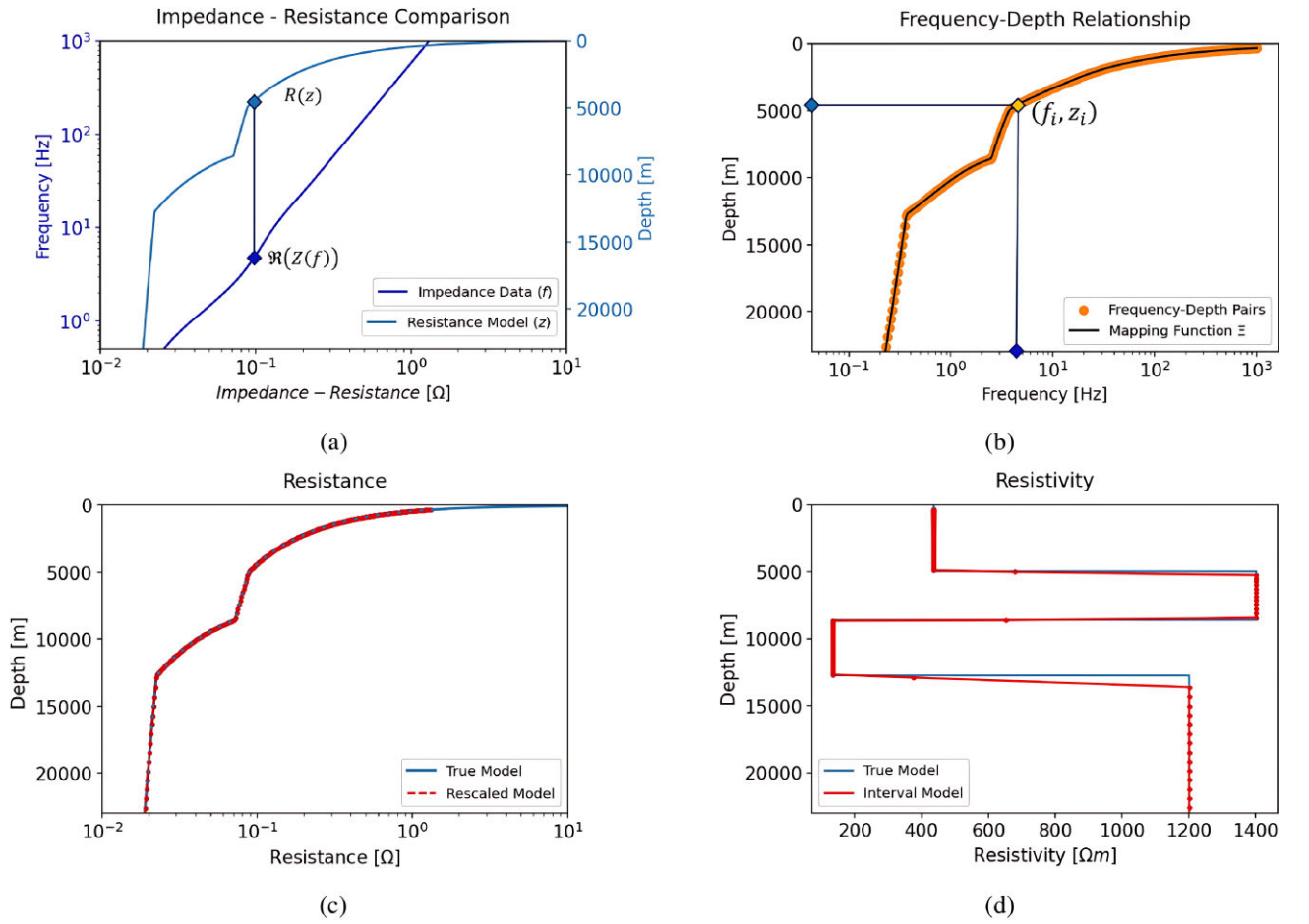

Figure 1. Data and model matching for a given data point (a), frequency-depth pairs for all m data points and the mapping function Ξ between data and model (b). the rescaled data in the resistance domain (c), the interval and true resistivity models (d).

and then into interval resistivity models, validating the approach for the direct transformation of MT data into 1-D resistivity models.

2 METHOD

To outline the method, we simulated synthetic MT data from a 1-D resistivity model (Fig. 1d, blue) by using the forward modelling routine *empymod* provided by Werthmüller (2017).

In the 1-D case of the MT method from one simulated horizontal component of the magnetic field transformed to the frequency domain, for example $H_y(f)$, and the corresponding orthogonal electric field component, $E_x(f)$, we may obtain the plane wave impedance $Z_{xy}(f)$ as

$$Z_{xy}(f) = \frac{E_x(f)}{H_y(f)}. \tag{1}$$

To relate the computed impedance data to the model of the subsurface we used a cumulative model starting from a layered resistivity model, the concept of cumulative resistance $R(z)$ is used and computed from the longitudinal conductance $S(z)$ to arrive at a monotonically decreasing resistance model function of depth z. This cumulative formulation of the layered model allows a one-to-one correspondence with the impedance data. In contrast, the concept of apparent resistivity does not allow a unique mapping as a given apparent resistivity value may be located at multiple depths. The cumulative resistance, $R(z)$ is given by

$$R(z) = \frac{1}{S(z)}, \tag{2}$$

where

$$S(z) = \sum_{i=1}^{n} \frac{h_i}{\rho_i} + \frac{(z - z_n)}{\rho_{i+1}} \quad \text{for} \quad z_n < z < z_{n+1} \tag{3}$$

with ρ_i being the resistivity of layer i, h_i the thickness of layer i and $i = 1, ..., N$ where N is the number of layers in the model.

For each point in the simulated data, using the real component of the complex impedance $\Re(Z_{xy}(f_i))$ and the resistance model $R(z)$, we search in the cumulative model for the point in depth at which $\Re(Z_{xy}(f_i))$ is equal to the cumulative resistance $R(z)$ as

$$z_i = \arg_z \left[R(z) = \Re(Z_{xy}(f_i)) \right] \tag{4}$$

(Fig. 1a), which required interpolating the resistance model to ensure a mapping for all data points. This process associates each data frequency f_i with a corresponding depth z_i leading to m data–model pairs (f_i, z_i) that define the mapping function Ξ (Fig. 1b) that directly rescales the MT data measured at a given frequency to its corresponding point in depth in the resistance model as $\hat{z} = \Xi(f)$, where $\hat{z}$ denotes the rescaled depth.

If the mapping function Ξ is known, it can be applied to the impedance data to rescale them into a cumulative resistance model by mapping the impedance values from the data domain (f) to the

Downloaded from https://academic.oup.com/gji/article/244/1/ggaf425/8300377 by guest on 19 November 2025

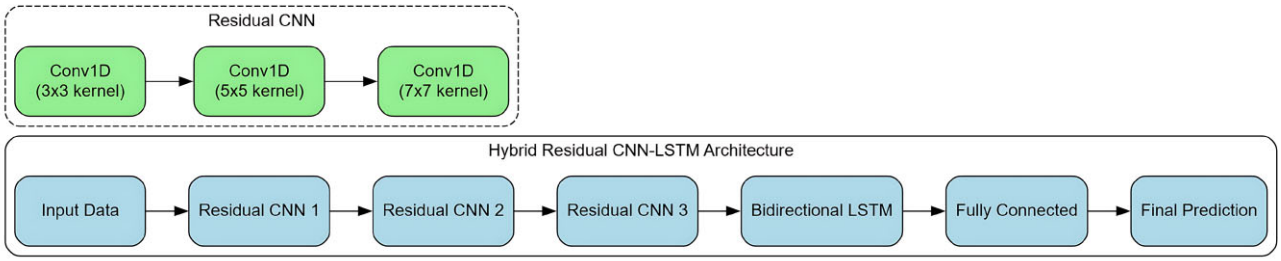

Figure 2. Proposed architecture for our custom neural network model.

model domain (z) (Fig. 1c). Once the data has been rescaled into a resistance model the interval resistivity model is retrieved (Fig. 1d) by differentiating eq. (2) as

$$\rho_i = \frac{h_i}{\frac{1}{R(z_i)} - \frac{1}{R(z_{i-1})}} = \frac{z_i - \sum_{j=1}^{i-1} h_j}{\sum_{j=1}^{i} \frac{h_j}{\rho_j} - \sum_{j=1}^{i-1} \frac{h_j}{\rho_j}}. \tag{5}$$

The resistivity model retrieved from the discretization of the rescaled resistance model is referred to as *Interval Resistivity Model* to differentiate it from the resistivity model used to simulate the MT data.

To compute the Ξ function from the data, we designed a custom convolutional–long short term memory (CNN-LSTM) neural network (Wei *et al.* 2021; Liao *et al.* 2022; Maiti & Chiluvuru 2024) trained to generalize the behaviour of the model–data relationship. The rescaling process was defined as

$$\hat{z} = \hat{\Xi}\left(\Re(Z_{xy}(f)), \phi(f), f\right) \quad \text{with} \quad \Re(Z_{xy}(f)) = R(z), \tag{6}$$

taking as input parameters the real part of the 1-D impedance data $\Re(Z_{xy}(f))$, the phase of the data $\phi(f)$ and the frequency at which the data were measured f and the output parameter was defined to be the rescaled depth $\hat{z}$. Although the mapping function Ξ was established using only the real component of the impedance data, the network receives the full complex impedance, represented by its real and phase components, encoding the information present in the data. $\hat{\Xi}$ denotes the rescaling process performed by the neural network. The general structure of the network is shown in Fig. 2.

Within the residual CNN block depicted in Fig. 2 each convolutional block was designed to include padding to preserve the size of the input features and a ReLU activation function was used for each residual CNN block. The results of the bidirectional LSTM and fully connected layers were used without imposing further activation functions. For our custom CNN-LSTM network we implemented a custom weighted loss function and used Adam as optimizer. Our loss function was defined as

$$\mathcal{L} = \sqrt{\frac{\sum_{i=1}^{m} w_i (y_{\text{True}_i} - y_{\text{Pred}_i})^2}{\sum_{i=1}^{m} w_i}}, \tag{7}$$

where the weight w_i is calculated based on the number of points per each decade in depth as

$$w_i = \frac{1}{n_{d(i)}} \tag{8}$$

with n being the number of points in the current decade and $d(i)$ the decade corresponding to point i.

For training and validation of the network, we generated a data set of 20 000 random resistivity models; where the parameters of each model could vary randomly according to Table 1; for each resistivity model we defined a set of survey parameters that varied according to Table 1 and simulated the MT data using the aforementioned Python routine. Subsequently, for each model-data pair, we recovered the rescaled depth $\hat{z}$ when $\Re(Z_{xy}(f)) = R(z)$.

Table 1. Parameters of the training data set.

Model parameters	
Number of layers: 4–10	
Resistivity range (Ωm): $1 \times 10^{-1} - 5 \times 10^{3}$	
Thickness range (m): 5×10^{2}–1×10^{4}	
Survey parameters	
Frequency band (Hz): $1 \times 10^{-4} - 1 \times 10^{3}$	
Number of samples: 50–500	
Type of f spacing: Lin–Log	

In the training phase, the data set was randomly divided into two subsets, the training set which contained 80 per cent of the original 20 000 models and the validation set which contained the remaining 20 per cent. The training phase took 12 hr for 819 epochs using an AMD EPYC 7742 CPU and a Nvidia A100 GPU, while the rescaling of the validation data set using the trained network took 7.5 min with an AMD Ryzen 7 3800H CPU and a Nvidia RTX 3060 GPU.

3 RESULTS

3.1 Synthetic MT data

To assess the rescaling capabilities of the trained network for unseen data; we rescaled the MT data of the validation data set and retrieved the interval resistivity model by applying eq. (5). To evaluate the goodness of the results we computed the mean absolute percentage error (MAPE). We use it for the true and rescaled resistance models, the true and retrieved interval resistivity models and the real component of the impedance data $\Re(Z_{xy}(f))$, referred to as *measured data* and the impedance data simulated using the retrieved interval resistivity model. The MAPE error is defined as

$$\text{MAPE per cent} = \frac{1}{n} \sum_{\text{i}}^{n} \frac{|\text{y}_{\text{True}} - \text{y}_{\text{Pred}}|}{\text{y}_{\text{True}}} \cdot 100 \,\text{per cent}, \tag{9}$$

where y_{True} corresponds to the true value and y_{Pred} corresponds to the value retrieved from the method.

For comparison with a 1-D inversion, we trained a second neural network ($\hat{\Theta}$) using the architecture depicted in Fig. 2 to solve a classical inversion problem for MT data. This inverting network $\hat{\Theta}$ (which results will be referred to as *inverted*) was trained using the same 20 000 model data set giving as input parameters $\Re(Z_{xy}(f))$, $\phi(f)$ and f and setting as output parameters the resistivity model (ρ, z) with a number of layers equal to the number of data points m in each profile. Additionally, for comparison with known data-driven inversions, we computed the Niblett–Bostick transformation (referred to as *N-B*) and the updated version of Niblett–Bostick

Downloaded from https://academic.oup.com/gji/article/244/1/ggaf425/8300377 by guest on 19 November 2025

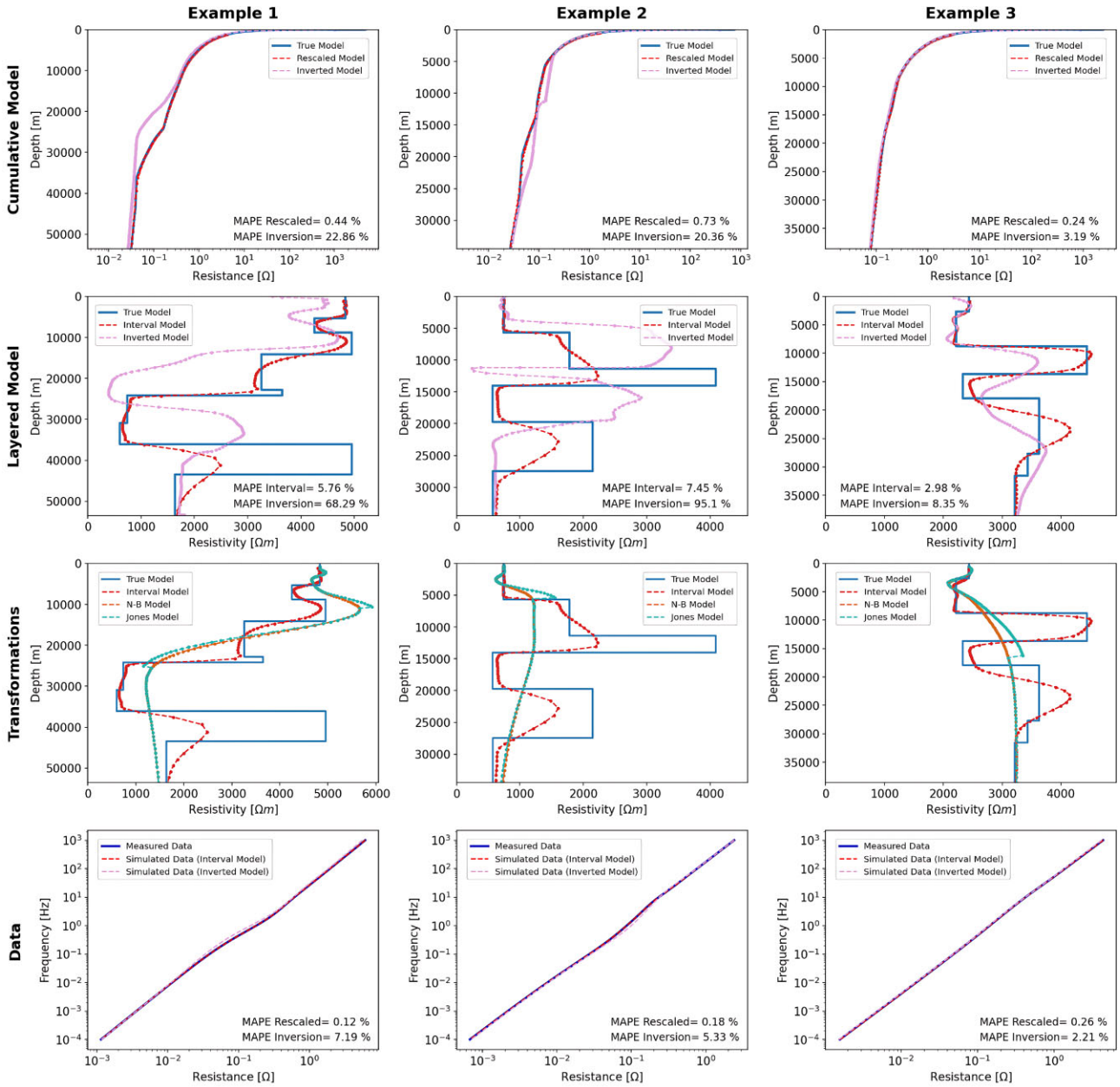

Figure 3. Rescaling, inversion results from the same network architecture and direct data transformation results for three synthetic MT data profiles randomly selected from the validation data set.

derived by Jones & Foster (1986) (referred to as *Jones*) for the MT data in the validation data set.

In Fig. 3 we present the comparison between the results retrieved by our method (red), the results retrieved by the inverting network $\hat{\theta}$ (pink) and the true model (blue) as follows; the first row compares the rescaled resistance model (red), the resistance model computed from the inverted resistivity model (pink) and the true resistance model (blue). The second row presents the interval resistivity model, the inverted resistivity model and the true resistivity model. The third row presents the comparison between the interval resistivity model and the resistivity models retrieved by the N-B (orange) and Jones (light green) transformations with the true resistivity model. The fourth row displays the simulated data computed from the interval resistivity model, the simulated data computed from the inverted resistivity model, and the measured data computed using the true resistivity model.

The results show that it is possible to rescale synthetic 1-D MT data into a resistance model, which can then be turned into an interval resistivity model. The overall misfit for the validation data set was as follows: the MAPE for the rescaled resistance model varies from 0.1 per cent to 5 per cent and the interval resistivity has an overall misfit between 1 and 20 per cent compared to the real resistivity model. The MAPE for the simulated data computed from the interval resistivity model ranges from 0.01 per cent to 3 per cent, which implies that the recovered interval resistivity models can be considered valid solutions of the inverse problem. Furthermore, the results show that even if the data and the cumulative resistance model are smooth, the transformation of the rescaled resistance model into an interval resistivity model recovers a blocky layered

Downloaded from https://academic.oup.com/gji/article/244/1/ggaf425/8300377 by guest on 19 November 2025

model. In the retrieved interval resistivity model, the position and thickness of the layers are estimated with good accuracy, the true resistivity is also estimated quite well in the portion of the model where the data are sensitive enough to model parameters. Hence, low resistivity layers are retrieved with greater accuracy than the high resistivity layers. Highly accurate results are obtained without the need of introducing *a-priori* information like, for example, the number of layers or the expected resistivity range of the model.

The rescaling neural network $\hat{\Xi}$, results are shown to be significantly better than those obtained with the inverting network, $\hat{\Theta}$. The use of cumulative models seems to reduce the nonlinearity of the inverse problem. The rescaling network Ξ retrieves the cumulative resistance model and we compute the interval resistivity model from it. The inverting network retrieves the interval resistivity model, and we can compute the cumulative resistance model from it. Both models from the rescaling network have significantly lower error than those from the inverting network. Furthermore, the data fit is considerably better by using the rescaling neural network. When using the interval resistivity recovered from the rescaled resistance model to simulate the MT data, the misfit between measured and simulated data is in the order of 0.01 per cent to 3 per cent; whereas, it is the range between 0.1 per cent to 20 per cent when using the inverted resistivity model for the validation data set.

The third row in Fig. 3 shows the resistivity models retrieved by direct data transformations based on apparent resistivity and skin depth. The resistivity models retrieved by N-B and Jones are almost equal; however, differences between these two approaches arise when transitioning to layers with higher resistivities because the Jones transformation was built to compensate for the diminished sensitivity of the MT data when transitioning to higher resistivities. Nonetheless, the results show that both transformations replicate the behaviour of the apparent resistivity as function of depth, whereas the results retrieved by the cumulative resistance model approach of the rescaling neural network $\hat{\Xi}$ provide realistic models with high resolution, without imposing assumptions on the data.

3.2 COPROD2 Data set

To evaluate the practical applicability of our method for measurements collected in the field, we used the COPROD2 data set (Jones 1993) which comprises 35 stations along a 400 km east–west profile that crosses the North American Central Plains (NACP) conductivity anomaly in Saskatchewan and Manitoba, Canada. The COPROD2 data set, available on the site MTNet, serves as a benchmark for new methodologies in MT processing and inversion due to its complex geological settings that generate important 2-D features in MT data. Although, the proposed method is at the present stage 1-D, we applied it to the COPROD2 data with the aim of defining the overall resistivity distribution and to compare it with the wide set of models retrieved with classical local and global search inversion methods. The resistivity model is characterized by a conductive layer (1–10 Ωm) in the first 2–3 km, overlying a more resistive layer (10–1000 Ωm) down to a depth of 10–20 km. The NACP is expected at 10–15 km below stations E4-13 and the resistivity values of the NAPC anomaly, associated with graphitic sheets in highly metamorphosed rocks, are expected to be in the range 0.1–10 Ωm according to what has been described by Jones *et al.* (2005).

Like other works, we used only 20 stations that belong to the central part of the profile in which the NACP can be located. We chose not to remove the high frequency part of the measurements, contrary to what was suggested by Jones (1993) to reduce the dimensionality of the 2-D inverse problem. Since the training of our network was carried out with a minimum number of 50 data points, we interpolated the TE mode data such that we had 50 frequency samples for every station and then rescaled the data into cumulative resistance models which were discretized into interval resistivity models. As with the synthetic test, we assessed the quality of the rescaled profiles by simulating the data for each station using the retrieved interval resistivity model as input. We then computed MAPE of the simulated TE mode data using the computed interval layered model.

Fig. 4(a) presents the retrieved resistivity section as a sequence of the retrieved 1-D resistivity models. The highly conductive layer is clearly visible in the first 3 km of the section. In the 2-D inversion results presented in literature, this layer is usually assumed as *a priori* information retrieved by the 1-D inversion of the high frequency data that was subsequently removed from the data (Degroot-Hedlin & Constable 1993; Pace *et al.* 2021). Furthermore, a low-resistivity anomaly is present at 20 km below stations 01–13 which is in agreement with the results described by several authors (e.g. Pace *et al.* 2021; Song *et al.* 2022; Peng *et al.* 2024). The MAPE of the data misfit for the computed impedance from the data and the data simulated from the interval resistivity models, has an average value of 7.7 per cent, which is in agreement with the results retrieved by Degroot-Hedlin & Constable (1993). In general, our resistivity model aligns well with other models obtained through 2-D inversions (Degroot-Hedlin & Constable 1993; Pace *et al.* 2021; Peng *et al.* 2024), despite its limitation in resolving the detailed structure of the NACP conductive anomaly. Furthermore, our model is consistent with the expected 1-D anomalies described by Jones (1993). The results obtained for the COPROD2 data set were retrieved in 7.83 s using the same equipment as for the rescaling of the validation data set, highlighting the efficiency and low computational cost of our method compared to other inversion processes. Given the minimal running time required to retrieve a plausible resistivity model, our interval resistivity models are well-suited to be used as data-driven reference models for 2-D or 3-D inversion processes, expecting to reduce the solution space and convergence time.

In general, the results show that even though the rescaling network was trained with a limited number of samples and only on 20 000 models it can produce accurate interval resistivity models. However, re-training is recommended if the expected resistivities or the frequency band of the data extend beyond those covered by the training data set (Table 1). Furthermore, the rescaling capabilities of the network are constrained to the training data set used and the appropriateness of the 1-D medium assumption. These intrinsic limitations can be overcome by widening the model space of the training data set and finding an adequate mapping procedure in two dimensions.

4 CONCLUSIONS

We have demonstrated that we can rescale MT impedance data into a 1-D cumulative resistance model by a mapping function Ξ in a neural network between the $\Re(Z_{xy}(f))$, $\phi(f)$ and f of MT data and a model. This approach is fully data driven, without the need of *a-priori* information. The results show that by using cumulative models the nonlinearity of the inversion problem seems reduced compared with a conventional inversion. This was demonstrated by using two networks that have the same architecture and that are trained with the same data set. Furthermore, our method provides more accurate results compared to other direct data transform

Downloaded from https://academic.oup.com/gji/article/244/1/ggaf425/8300377 by guest on 19 November 2025

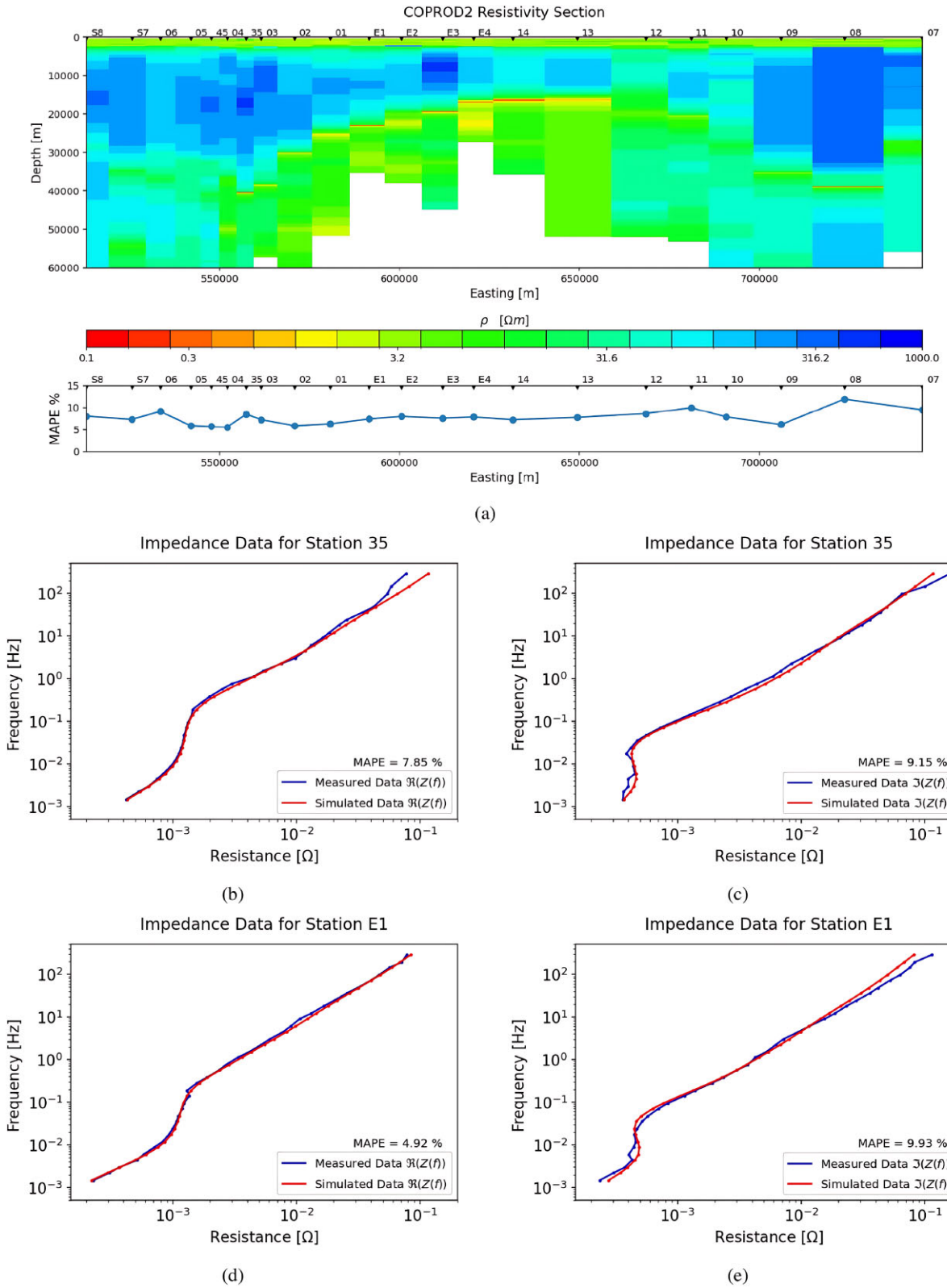

Figure 4. The resistivity section recovered by rescaling the data of all the stations with the mean MAPE for the simulated complex impedance for each station (a), the simulated and measured real and imaginary parts of the computed impedance for station 35 (b,c) and for station E1 (d,e).

approaches that rely on the concept of apparent resistivity and skin depth.

The field data results show features that agree with the anomalies expected in the area. However, due to the intrinsic 1-D nature of our method, our resistivity model fails to recover the fine details of the NACP anomaly. Nevertheless, the data misfit between the measured and predicted data show that the error is within the same range of the data fitting of published 2-D inversion results, indicating

Downloaded from https://academic.oup.com/gji/article/244/1/ggaf425/8300377 by guest on 19 November 2025

that our model can be regarded as a valid representation of the subsurface.

Overall, our method represents a promising tool for MT studies where 1-D features are to be expected. Moreover, the interval resistivity models retrieved by our method can be used as initial models for 2-D or 3-D inversions that are purely data-driven. Further research will focus on developing a 2-D approach of the method described in this work.

ACKNOWLEDGMENTS

We would like to thank the editor, Lindsey Heagy and the reviewer Anton Ziolkowski for their thorough review of the first version of this paper and their constructive comments that helped us improve our paper.

LR, as member of GNFM (Gruppo Nazionale per la Fisica Matematica) of INdAM (Istituto Nazionale di Alta Matematica), acknowledges that this work has been performed under the auspices of GNFM of INdAM. LR has been partly funded under the project NODES, from the MUR-M4C2 1.5 of PNRR funded by the European Union—NextGenerationEU (Grant agreement no. ECS00000036).

This work was performed using the computational facilities provided by the Department of Geoscience Engineering of TU Delft.

DATA AVAILABILITY

The python routine *empymod* used to simulate the synthetic MT data for 1-D resistivity profiles provided by Werthmüller (2017) is publicly available, detailed instructions on the use of the routine can be found at https://empymod.emsig.xyz/en/stable/index.html.

The COPROD2 data set (Jones 1993) is publicly available and can be downloaded from the MTnet site: https://www.mtnet.info/data/coprod2/coprod2.html.

The specific architecture of the neural network is publicly available in Zenodo at https://doi.org/10.5281/zenodo.15480937.

REFERENCES

Bailey, R.C., 1970. Inversion of the geomagnetic induction problem, *Proc. R. Soc. London. A. Math. Phys. Sci.,* **315**(1521), 185–194.

Constable, S.C., Parker, R.L. & Constable, C.G., 1987. Occam's inversion: A practical algorithm for generating smooth models from electromagnetic sounding data, *Geophysics,* **52**(3), 289–300.

Degroot-Hedlin, C. & Constable, S., 1993. Occam's inversion and the North American Central Plains electrical anomaly, *J. Geomagn. Geoelectr.,* **45**(9), 985–999.

Florio, G., 2018. Mapping the depth to basement by iterative rescaling of gravity or magnetic data, *J. geophys. Res.: Solid Earth,* **123**(10), 9101–9120.

Grandis, H., Menvielle, M. & Roussignol, M., 1999. Bayesian inversion with Markov chains—I. The magnetotelluric one-dimensional case, *J. geophys. Int.,* **138**(3), 757–768.

Jones, A.G., 1993. The COPROD2 data set: tectonic setting, recorded MT data, and comparison of models, *J. Geomagn. Geoelectr.,* **45**(9), 933–955.

Jones, A.G. & Foster, J.H., 1986. An objective real-time data-adaptive technique for efficient model resolution improvement in magnetotelluric studies, *Geophysics,* **51**(1), 90–97.

Jones, A.G., Ledo, J. & Ferguson, I.J., 2005. Electromagnetic images of the Trans-Hudson orogen: the North American Central Plains anomaly revealed, *Can. J. Earth Sci.,* **42**(4), 457–478.

Liao, X., Zhang, Z., Yan, Q., Shi, Z., Xu, K. & Jia, D., 2022. Inversion of 1-D magnetotelluric data using CNN-LSTM hybrid network, *Arab. J. Geosci.,* **15**(17), 1430.

Maiti, S. & Chiluvuru, R. K., 2024. A deep CNN-LSTM model for predicting interface depth from gravity data over thrust and fold belts of North East India, *J. Asian Earth Sci.,* **259,** 105881.

Niblett, E.R. & Sayn-Wittgenstein, C., 1960. Variation of electrical conductivity with depth by the magneto-telluric method, *Geophysics,* **25**(5), 998–1008.

Pace, F., Santilano, A. & Godio, A., 2021. A review of geophysical modeling based on particle swarm optimization, *Surv. Geophys.,* **42**(3), 505–549.

Peng, R., Han, B., Hu, X., Li, J. & Liu, Y., 2024. 2-D probabilistic inversion of MT data and uncertainty quantification using the Hamiltonian Monte Carlo method, *J. geophys. Int.,* **237**(3), 1826–1841.

Rodriguez, O., Taylor, J.M. & Pardo, D., 2023. Multimodal variational autoencoder for inverse problems in geophysics: application to a 1-D magnetotelluric problem, *J. geophys. Int.,* **235**(3), 2598–2613.

Socco, L.V. & Comina, C., 2015. Approximate direct estimate of *S*-wave velocity model from surface wave dispersion curves, in *Near Surface Geoscience 2015–21st European Meeting of Environmental and Engineering Geophysics, Vol. 2015,* Turin, Italy, pp. 1–5.

Socco, L.V., Comina, C. & Anjom, F.K., 2017. Time-average velocity estimation through surface-wave analysis: Part 1—*S*-wave velocity, *Geophysics,* **82**(3), U49–U59.

Song, H., Yu, P., Wang, C., Zhang, L., Zhao, C., Shi, B. & Hu, M., 2022. 2D magnetotelluric inversion using hybrid stabilizing functionals: exponential minimum support and smoothness, *Geophysics,* **87**(5), E307–E317.

Tikhonov, A.N., 1965. Mathematical basis of the theory of electromagnetic soundings, *USSR Comput. Math. Math. Phys.,* **5**(3), 207–211.

Trainor-Guitton, W. & Hoversten, G.M., 2011. Stochastic inversion for electromagnetic geophysics: practical challenges and improving convergence efficiency, *Geophysics,* **76**(6), F373–F386.

Wang, H., Liu, Y., Yin, C., Li, J., Su, Y. & Xiong, B., 2022. Stochastic inversion of magnetotelluric data using deep reinforcement learning, *Geophysics,* **87**(1), E49–E61.

Wei, C., Xue-Bao, G., Feng, T., Ying, S., Wei-Hong, W., Hong-Ri, S. & Xuan, K., 2021. Seismic velocity inversion based on CNN-LSTM fusion deep neural network, *Appl. Geophys.,* **18**(4), 499–514.

Werthmüller, D., 2017. An open-source full 3D electromagnetic modeler for 1D VTI media in Python: empymod, *Geophysics,* **82**(6), WB9–WB19.

Zhang, Y. & Paulson, K.V., 1997. Magnetotelluric inversion using regularized Hopfield neural networks, *Geophys. Prospect.,* **45**(5), 725–743.

Downloaded from https://academic.oup.com/gji/article/244/1/ggaf425/8300377 by guest on 19 November 2025

© The Author(s) 2025. Published by Oxford University Press on behalf of The Royal Astronomical Society. This is an Open Access article distributed under the terms of the Creative Commons Attribution License (https://creativecommons.org/licenses/by/4.0/), which permits unrestricted reuse, distribution, and reproduction in any medium, provided the original work is properly cited.